MULTISCIA
JOURNALS PUBLISHERS

FRONTIERS IN PHARMACEUTICAL ANALYSIS

ISSN: (3065- 1352)

https://multisciajournals.com/journals/index.php/fpa
editor.fpa1@gmail.com

Frontiers in Zoological Research
Volume 1 Issue 2 2025

The dorsal raphe nucleus contains dopaminergic neurons that may influence social dominance in mice.

SS Tangeda, LBM Neti
Department of **Zoological Research**

Article Info

Received: 30-4-2025 Revised:08-06-2025 Accepted:19-06-2025 Published:29-06-2025

ABSTRACT

Individual physiology, behavior, and social interactions are shaped by social hierarchies, which are essential to the organizational framework of group-living animals. Although dopaminergic (DA) systems have been connected to motivation and competitive behaviors, especially in the dorsal raphe nucleus (DR) and ventral tegmental area (VTA), their region-specific roles in social dominance are still unclear. In sexually naïve male C57BL/6J mice, this study examined the function of VTA and DR DA neurons in controlling social dominance. Following the establishment of stable hierarchies using the tube test, both dominant and subordinate mice showed increased expression of c-Fos in the VTA and DR. Interestingly, c-Fos activation in DR DA neurons was noticeably higher in dominant animals than in subordinates. Fiber photometry showed that DR neurons were more strongly engaged during dominance-related acts, while DA neurons in both regions were suppressed during passive retreats and activated during proactive push behaviors. In dominant mice, chemogenetic suppression of DR DA neurons decreased their social rank, but in subordinate mice, activation increased their rank. On the other hand, social dominance was not significantly affected by chemogenetic manipulation of VTA DA neurons. Certain anxiety-like behavioral traits changed in a rank-dependent manner when DA neurons in both regions were manipulated. These results demonstrate the different functions of DR and VTA DA neurons in the regulation of social hierarchy, highlighting DR DA neurons as a key element in the control of social dominance.

Keywords: dopamine, ventral tegmental region, dorsal raphe nucleus, social hierarchy, and chemogenetics

Introduction

Introduction: In group-living animals, dominance hierarchies are a distinguishing characteristic of social organization (Qu et al., 2017). They function as a social framework and a crucial regulatory mechanism that controls resource distribution and preserves group stability (Leclair & Russo, 2021). Individual fitness is significantly impacted by these hierarchies, resulting in a noticeable welfare imbalance (Johnson et al., 2012). According to Uchida et al. (2022), dominant people usually have preferred access to basic resources like food, shelter, and mating opportunities, which benefits their physical well-

being and ability to procreate. Conversely, subordinate people endure ongoing psychological stress, which puts them at risk for a variety of physiological and psychopathological conditions (Madigan & Daly, 2023). In addition to providing insight into basic ethological processes, this dichotomy highlights the neurobiological significance of social hierarchy and informs translational approaches to mental health illnesses (Battivelli et al., 2024b; Dwortz et al., 2022). Dopamine (DA), serotonin (5-HT), oxytocin, and steroid hormones are among the neuromodulatory systems that have been linked to the formation and upkeep of social hierarchies (Janet et al., 2022; Liu et al., 2025; Zhou et al., 2018). Among them, the DA system has become a crucial modulator of competitive outcomes because to its tight association with reward and motivation (Amaral et al., 2021). Dopaminergic projections from the nucleus accumbens (NAc) to the ventral tegmental area (VTA) in rats are important factors in determining social competition success (van der Kooij et al., 2018). Similar to humans, dominant nonhuman primates have higher levels of DA metabolites in their CSF fluid (Kaplan et al., 2002), and striatal dopamine D2/3

Accepted: May 26, 2025; Online: May 27, 2025; Received: April 13, 2025 Items for the foundation: The Natural Science Foundation of Henan Province (252300420211 to Y.J.L.); STI2030-Major Projects (2022ZD0205101 to F.D.T.); the National Natural Science Foundation of China (32270529 to L.F.L.; 32270510 to F.D.T.); and the Key Scientific Research Project of Higher Education Institutions in Henan Province (23A180001 to L.F.L.) provided support for this work.
#Equal contributions were made by the authors. *Corresponding authors' email addresses are taifadao@snnu.edu.cn and lilaifu@snnu.edu.cn.
According to Martinez et al. (2010), there is a positive correlation between receptor binding and social status.
The substantia nigra, VTA, and dorsal raphe nucleus (DR) are the main locations for DA neurons, each of which has unique projection targets and functions. The dorsal striatum is innervated bysubstantia nigra DA neurons, which are crucial for motor function (Tenchov et al., 2025). VTA DA neurons modulate emotion, motivation, memory, and reward-related behavior by projecting widely to limbic and forebrain areas (Garritsen et al., 2023; Lin et al., 2021). According to recent research, dominant mice actually show decreased dopaminergic activity in the VTA (Battivelli et al., 2024b), despite the fact that optogenetic activation of VTA DA neurons increases dominance in rats in competitive circumstances (Lozano-Montes et al., 2019). Furthermore, it has been demonstrated that social defeat in mice is encoded via projections from the medial prefrontal cortex (mPFC) to the VTA (Choi et al., 2024). There is growing evidence that DR DA neurons are a distinct subpopulation with specialized projection patterns that mainly target the central amygdala (CeA) and bed nucleus of the stria terminalis (BNST). These neurons have functional implications in arousal modulation, memory processing, sociability, and behaviors related to depression (Cho et al., 2017; Lin et al., 2020, 2021; Matthews et al., 2016; Wang et al., 2024). To our knowledge, the function of DR DA neurons in social rivalry has not been thoroughly investigated despite these correlations. The roles of DR and VTA DA neurons to the control of social hierarchy in mice were investigated in this work. After tube test evaluations in triad-housed cohorts, post-test c-Fos expression profiles in these neuronal populations were measured. Chemogenetic alterations were used to ascertain the causative effects on social ranking, and real-time calcium imaging was utilized to track neural activity during competitive interactions. In light of the DA system's well-established functions in social behavior and emotional regulation (Liu et al., 2021; Torquet et al., 2018), social preference and anxiety-like behaviors were also assessed during testing. The findings showed that bidirectional modulation of DR DA neurons changed dominance status and that these neurons were more activated in dominant animals following the tube test. However, rank was unaffected by changes in VTA

DA neuronal activity. These results imply that in mice, DR DA neurons have a greater impact on social dominance than VTA DA neurons. Our research offers fresh perspectives on how social hierarchy is represented in the brain, which has important ramifications for welfare and health.

SUPPLIES AND TECHNIQUES

Animals

Male C57BL/6J sexually naïve mice weighing 25–28 g and aged 8–10 weeks were acquired from Huaxing Experimental Animal Farm in Zhengzhou, China. In each cage, mice were kept in groups of three (26 cm length by 20 cm wide by 14 cm high) with unlimited access to food and water under regular circumstances (22±3°C, 12 h:12 h light/dark cycle, lights on at 0700 h). The Nanyang Normal University Animal Ethics Committee authorized all experimental techniques in accordance with the Chinese Guidelines for Laboratory Animal Care and Use (Protocol #202306010003). Unless otherwise noted, only dominant or subordinate mice were subjected to experimental interventions; intermediate-ranked mice were kept as undisturbed controls for social hierarchy evaluation.

Behavioral assessments

Every behavioral test was carried out in low light between 0900 and 1400 hours. Thirty minutes before each session, the mice were acclimated to the testing room. Unless otherwise noted, SuperMaze Systems (Shanghai Xinruan, China) was used to analyze the video recordings of the tests. Between sessions, the apparatuses were cleaned with 30% ethanol and patted dry with paper towels.

Tube test: The tube test was used to assess social dominance in mice (Fan et al., 2019; Li et al., 2023). Only one mouse at a time could pass through the clear tube, which was 30 cm in length and 3.5 cm in internal diameter. Over the course of three days, each mouse was trained to move through the tube five times a day. Cage-mates were taught in pairs for three more trials during the testing phase, and they were then evaluated in dyadic encounters using a round-robin approach. One mouse was positioned at each end of the tube and permitted to meet in the center of each trial. The meeting ended when one mouse pushed the other mouse out of the tube entirely. The "winner" was the mouse that advanced, while the "loser" was the mouse that retreated. Trials that lasted more than five minutes were stopped and rescheduled. Subsequent tests were limited to cages that had stable social hierarchies for at least four days in a row. Each cage was given a top (rank 1), middle (rank 2), and bottom (rank 3) hierarchical rank.

OFT, or open-field test: Locomotor activity and anxiety-like behavior were evaluated using the OFT (Zhou et al., 2024). An opaque plastic box of 50 cm in length, 50 cm in width, and 50 cm in height made up the apparatus. The floor was essentially divided into 16 equal quadrants, with the middle zone being defined by the four central quadrants. Each mouse was given its own space in the box and given five minutes to explore during the test. Both the overall distance traveled and the amount of time spent in the center zone were automatically recorded.

EPM, or elevated plus maze test: Two open arms (35 cm long by 5 cm wide by 1 cm high) and two closed arms (35 cm long by 5 cm wide by 15 cm high) that extended from a central platform (5 cm long by 5 cm broad) made up the EPM equipment. The maze was raised 70 centimeters off the ground. For five minutes, mice were left to roam freely on the middle platform while facing an open arm. For analysis, the quantity of entries and amount of time spent in each arm were noted.

Test of social interaction (SI): The SI test (Wang et al., 2022) was used to assess sociability in the same open-field box apparatus as previously mentioned. On one side of the box, a wire mesh cage measuring 11 cm in height by 9 cm in diameter was positioned in the middle. An interaction zone (30 cm long by 20 cm around the wire cage) and a non-interaction zone were virtually separated on the floor. There were two 5-minute trials throughout the test. The wire mesh cage was empty for the initial "target-absent" trial. A new C57BL/6J male mouse was introduced into

the wire mesh cage for the second "target-present" session. During both experiments, the amount of time spent in the interaction and non-interaction zones was noted. The SI ratio, which is calculated by dividing the amount of time spent in the interaction zone during the target-present trial by the amount of time spent there during the target-absent trial, was used to quantify sociability.

The use of immunofluorescence

After the behavioral testing was finished, the next day, the Six successive tube test trials were performed on the animals. Mice were put to sleep with 2% sodium pentobarbital 90 minutes after the last trial. They were then transcardially perfused with 0.1 mol/L phosphate-buffered saline (PBS) and 4% paraformaldehyde (PFA). After being promptly removed, the brains were post-fixed in 4% PFA for three days and subsequently dehydrated in solutions of 15% and 30% sucrose. A cryostat (Leica CM1950, Germany) was then used to chop the brains into 40-μm coronal slices, which were subsequently placed onto glass slides covered with gelatin. The sections were then washed with PBS (5 min×3), blocked for two hours at room temperature with 5% normal goat serum, and then incubated with primary antibodies—mouse anti-tyrosine hydroxylase (TH, a rate-limiting enzyme in DA synthesis) (1:500, sc-25269, Santa Cruz, USA) and rabbit anti-c-Fos (1:2 000, ab190289, Abcam, UK)—for an entire night at 4°C. The sections were thoroughly cleaned with PBS (5 min×3) and then incubated for two hours at room temperature with secondary antibodies: goat anti-rabbit conjugated with TRITC (1:400, AB_2337932, Jackson, USA) and goat anti-mouse conjugated with 488 (1:400, 115545146, Jackson, USA). A ZEISS inverted fluorescence microscope Axio Observer 7 (Carl Zeiss AG, Germany) was used to image each section after it had been stained with DAPI for 10 minutes at room temperature and rinsed in PBS for 5 minutes by three. Three anatomically matched slices of the mouse brain covering rostral to caudal regions were used for the quantification of Fos-positive and TH-positive neurons. Consistency was ensured by employing consistent regions of interest (ROIs). To reduce variability, numbers from the three parts were averaged for each mouse. The number of TH/c-Fos double-labeled cells divided by the number of TH-labeled cells was used to determine the TH/c-Fos colocalization rate.

Vectors of viruses

AAV-TH-CRE-WPRE-hGH-polyA (Cat#: PT-2947, BrainVTA, China), AAV-EF1α-DIO-mCherry-WPRE-hGH-polyA (Cat#: PT-0013, BrainVTA, China), AAV-EF1α-DIO- hM3D(Gq)-mCherry-WPREs (Cat#: PT-0042, BrainVTA, China), AAV-EF1α-DIO-hM4D(Gi)-mCherry-WPREs (Cat#: PT-0043, BrainVTA, China), and AAV-TH-GCaMP6s-WPRE-hGH-

AAV-TH-eGFP- WPRE-hGH-polyA (Cat#: PT-0184, BrainVTA, China), and polyA (Cat#: PT-2148, BrainVTA, China). 3–4×1012/mL were the titer values.

Chemogenetic modifications and viral injection

Mice were put in a stereotaxic device (RWD Life Science, China) after being sedated by inhaling 1.5%–3.0% isoflurane. A 33-gauge syringe needle was used to stereotactically inject viral vectors into the intended areas once the skull was exposed (Hamilton, Switzerland). A 1:1 volumetric ratio was used to combine the Cre-expressing and DIO-AAV vectors, which were then injected at a rate of 100 nL/min to reach 600 nL. To avoid reflux, the syringe was left in place for five minutes after the infusion and then gradually removed. After surgery, the mice were put back in their original cages and kept there until the next set of tests. VTA: AP −3.2 mm, ML±0.5 mm, DV – 4.7 mm; DR: AP −4.0 mm, ML +0.2 mm, DV −3.3 mm were the target coordinates in relation to bregma. Three weeks following viral administration, behavioral evaluations started. Clozapine-N-oxide (CNO, Cat#: CNO-01, BrainVTA, China) was dissolved in 1% dimethyl sulfoxide (DMSO) and diluted with regular saline to reach a final concentration of 1 mg/mL for chemogenetic manipulation. The solutions were kept at

-20°C till in use. Mice were given a short anesthetic and an intraperitoneal injection of either

vehicle (Veh) or CNO (0.2 mL) thirty minutes before to behavioral assessment. 500 nL of either control AAV-TH-eGFP or fiber photometry AAV-TH-GCaMP6s was injected into the VTA or DR. An optical fiber with a core diameter of 250 μm was inserted 0.3 mm dorsal to the injection site three weeks after the injection and fastened with dental acrylic and a screw. One week following implantation, dominance ranking based on tube tests was established. A three-color single-channel fiber photometry device (ThinkerTech, China) was used for recordings in order to track Ca2+ signals in VTA and DR DA neurons. Green fluorescent signals of GCaMP6s were excited and recorded using a 470 nm laser light, and motion artifacts were corrected using a 405 nm signal as a control channel. At the end of the optic cable, the laser intensity was set to 40 μW, and the sampling frequency was set to 100 Hz in order to lessen the bleaching of GCaMP6s. Only mice with consistent hierarchical ranking were tested, and fiber photometry recordings were made in accordance with known protocols (Zhang et al., 2022). The device was made up of a modified 60-cm tube with two movable doors 15 cm from one end. To provide a baseline recording and reduce human handling interference, mice were kept in the tube before the door was opened. Within the open-field box, a side-mounted camera was used to record behavioral events. Three types were identified by behavioral annotation during analysis: retreating (voluntary withdrawal or displacement, usually with head lowering), pushing (making contact by pushing the head beneath an opponent), and walking alone (Fan et al., 2023). For every mouse, three to five instances of each behavior were recorded. Fluorescence traces were recorded two seconds prior to and three seconds following the initiation of each behavior in order to correlate them with behavioral onset. Subtracting the 405 nm signal from the 470 nm signal yielded ΔF/F, which may be expressed as (F−F0)/F0, where F0 is the baseline fluorescence signal averaged over a 1-s window between 5 and 4 seconds before to a particular behavioral event. The sum of the fluorescence changes across the behavioral epoch divided by its duration was used to compute the normalized area under the curve (AUC) values. If a postmortem investigation showed incorrect fiber placement or no viral expression, the subjects were not included in the analysis.

Analysis of data

When necessary, paired t-tests or independent samples were used for pairwise comparisons. One-way analysis of variance (ANOVA) was used to compare three or more groups, and two-way repeated-measures ANOVA was used to analyze multiple groups under various testing settings. Bonferroni correction was used in post-hoc analysis. Fisher's exact test was used to examine rank flipping rates. A significance level of $P<0.05$ was established. SPSS v.22.0 was used for all analyses. The figure legends include information on sample size and analysis techniques.

OUTCOMES

Social hierarchy traits and behavioral patterns among various rank groups

To evaluate social rank, the tube test was used.

formation and its persistence throughout time in male C57BL6/J mice kept in triads for a minimum of one week (Figure 1A–B). The majority of cohorts showed a stable hierarchical structure by the fourth testing day (Figure 1C). A quantifiable indicator of dominance behavior was a dominance score, which was computed as the average number of daily victories for each person across rank groups. $F(2,21)=49.650$, $P<0.010$; rank 1 vs. rank 2, rank 1 vs. rank 3, rank 2 vs. rank 3, all $P<0.010$) showed that rank 1 mice had considerably higher dominance scores than both rank 2 and rank 3 mice (Figure 1D). Exploratory activity and anxiety-like behavior were measured using the OFT, the conflict between natural fear and exploration was assessed using the EPM test, and friendliness was evaluated using the SI test in order to further investigate behavioral features linked to social rank. Figure 1E: $F(2,21)=0.016$, $P=0.984$; Figure 1F: $F(2,21)=0.064$, $P=0.938$; Figure 1G: $F(2,21)=0.029$, $P=0.880$; Figure 1H: $F(2,21)=0.450$, $P=0.643$; Figure 1I: $F(2,21)=0.018$, $P=0.982$; Figure 1J: $F(2,21)=0.109$, $P=0.897$).

After social rivalry, dominant mice have a selective increase in c-Fos expression in DR DA neurons.

TH and c-Fos double-labeling was used to measure neuronal activation in the VTA and DR after social rank competition in order to examine the role of DA signaling in the creation and maintenance of social hierarchies. Before immunostaining, mice in a control group passed through the tube six times without coming into contact with one another. Both dominant and subordinate mice in the VTA had considerably higher levels of c-Fos expression than controls (Figure 2G; $F(2, 18)=27.620$, $P<0.010$; dominants and subordinates vs. control, all $P<0.010$). Nevertheless, there was no significant difference between the groups in the percentage of c-Fos-positive TH-immunoreactive (c-Fos+TH+) neurons (Figure 2H; $F(2,18)=1.499$, $P=0.250$). After the tube test, the DR also showed increased c-Fos expression (Figure 2I; $F(2,18)=46.3$, $P<0.010$; dominants and subordinates vs. control, all $P<0.010$; dominants vs. subordinates, $P=0.016$). Additionally, dominant mice had a significantly greater proportion of c-Fos+TH+ neurons than both subordinates and controls (Figure 2J; $F(2,18)=38.24$, $P<0.010$, subordinates and controls vs. dominants, all $P<0.010$, subordinates vs. control, $P=0.028$). Both the VTA and the DR showed no discernible differences in TH+ neurons across groups (Supplementary Figure S1; VTA: $F(2,18)=0.130$, $P=0.880$; DR: $F(2,18)=0.240$, $P=0.790$).

proving that DA synthesis capacity is unaffected by social position. Together, these results show that although competitive encounters are linked to general neuronal activation in both the VTA and DR, dominant status is strongly associated with the selective recruitment of DR DA neurons, indicating a preferential role for this population in regulating social dominance.

When engaging in competitive push and retreat activities, the activity patterns of VTA and DR DA neurons are opposite.

During the tube test competition, real-time DA neuronal activity was recorded using in vivo fiber photometry. About 75% of GCaMP6s+ cells in the VTA and DR were co-labeled with TH, according to post-hoc histological analysis (Supplementary Figure S2).

When push behaviors began during competitive encounters, GCaMP6s fluorescence in both locations increased dramatically dropped during retreat behaviors, which led to a loss, and increased during winning behaviors (VTA: Figure 3E–G, I–K; DR: Figure 4D–F, H–J). AUC per second significantly increased during push epochs but significantly decreased during retreat epochs, according to quantitative analysis (Push: VTA, pre vs. post: $t(5)=5.175$, $P<0.010$, Figure 3G; DR, pre vs. post: $t(5)=9.280$, $P<0.010$, Figure 4F). Pre- and post-retreat: VTA ($t(5)=6.699$, $P<0.010$), Figure 3K; DR ($t(5)=4.299$, $P<0.010$), Figure 4J. While peak values did not differ substantially (VTA vs. DR, $t(10)=2.013$, $P=0.062$; Supplementary Figure

S3C), comparison between areas revealed that the DR had a significantly higher AUC per second than the VTA during push epochs (VTA vs. DR, t(10)=6.063, P<0.010; Supplementary Figure S3B). While the AUC per second showed a similar tendency without reaching significance (t(10)=2.214, P=0.051, Supplementary Figure S3E), DR neurons attained considerably lower valley values during retreat epochs than those in the VTA (VTA vs. DR, t(10)=2.590, P=0.027; Supplementary Figure S3F). When mice moved through the tube without an opponent, there were no discernible changes in the fluorescence of GCaMP6s (VTA: Figure 3M–O; DR: Figure 4L–N). Figure 4N: t(5)=0.252, P=0.811; Figure 3O: t(5)=1.069, P=0.334) or when competitive trials were undertaken by viral control animals (VTA: Figure 3H, L, P; DR: Figure 4G, K, O). Figure 3H: t(5)=1.424, P=0.214; Figure 3L: t(5)=1.433, P=0.211; Figure 3P: t(5)=0.385, P=0.716; Figure 4G: t(5)=0.036, P=0.973; Figure 4K: t(5)=0.493, P=0.643; Figure 4O: t(5)=1.193, P=0.286). These findings demonstrate that, as opposed to motion-induced artifacts, the recorded GCaMP6s signals represent actual neural activity associated with competitive behaviors. While chemogenetic modification of VTA DA neurons modifies certain anxiety-like behaviors, it has little effect on social dominance. Chemogenetics was used to bidirectionally modulate neuronal activity in order to evaluate the role of VTA neurons in social dominance. AAV-DIO-hM3D(Gq)-mCherry+AAV-TH-CRE, AAV-DIO-hM4D(Gi)-mCherry+AAV-TH-CRE, or control AAV-DIO-mCherry+AAV-TH-CRE were injected into the VTA of dominant and subordinate mice. Immunohistochemical examination revealed that 74.5% of mCherry+ cells co-expressed TH, while robust DREADD expression was found in the VTA (Figure 5C) (Supplementary Figure S4B). By intraperitoneally delivering CNO (1 mg/kg) and measuring c-Fos expression 90 minutes later, functional validation was carried out. Compared with controls, c-Fos+ neurons were significantly higher in hM3D(Gq) mice and lower in hM4D(Gi) mice (Supplementary Figure S4E, F; F(2,15)=37.320, P<0.010; hM3D(Gq) vs. Control, P<0.01, hM4D(Gi) vs. Control, P=0.017), confirming the efficacy of the viral strategy. Chemically altering VTA DA neurons in the tube test did not result in any discernible changes in dominance rank in either dominant or subordinate mice (dominance: hM3D(Gq)+Veh vs. hM3D(Gq)+CNO, rank change rate: 25%, Fisher's exact test, P=0.467, Figure 5E; hM4D(Gi)+Veh vs. hM4D(Gi)+CNO, rank change rate: 50%, Fisher's exact test, P=0.077, Figure 5F). Subordinates: hM3D(Gq)+Veh; hM4D(Gi)+Veh versus hM4D(Gi)+CNO; rank change rate: 37.5%, Fisher's exact test, P=0.2, Figure 5H Fisher's exact test, P=0.2, rank change rate: 37.5%, Figure 5I).

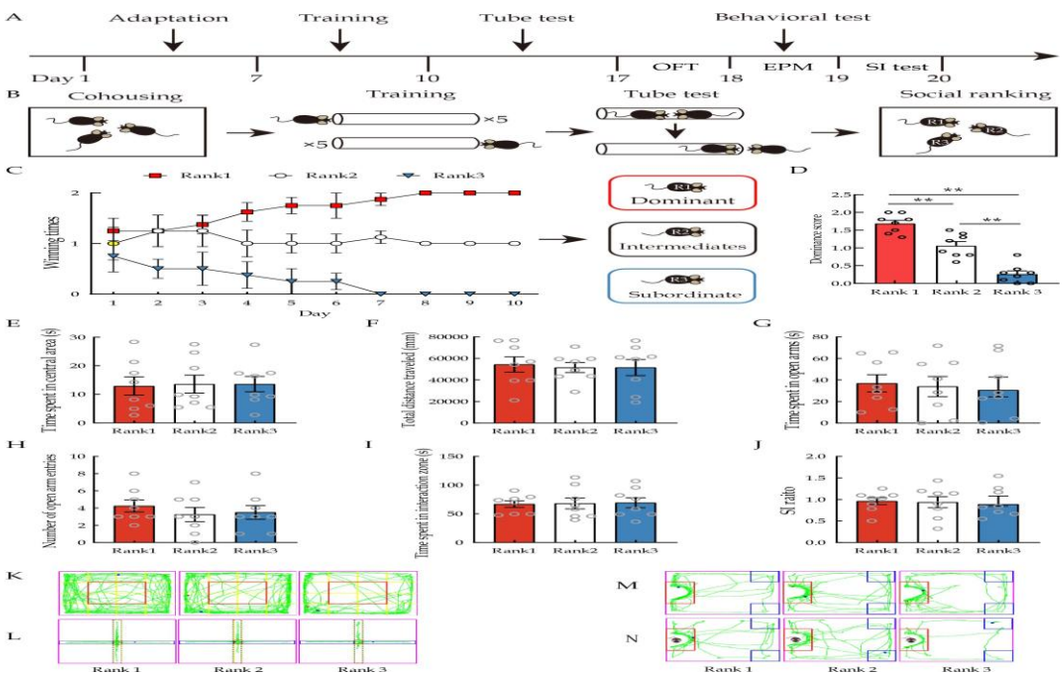

Figure 1 Social rank and behavioral performance

A: Study timeline. B: Schematic of the tube test. C: Social rank changes during training and the tube test. D: Dominance scores. Average number of wins per day across all days of the tube test is depicted for individuals categorized by rank. E, F: Time spent in the central zone and total distance traveled in OFT. G, H: Time spent in open arms and number of open arm entries in EPM test. I, J: Time spent in the interaction zone and SI ratio in SI test. K–N: Representative tracks in OFT, EPM, and SI test (upper panel: Target-absent trial; lower panel: Target-present trial). Data are presented as mean±SEM, analyzed by one-way ANOVA. n=8 in each group; *: P<0.050; **: P<0.010. EPM: Elevated plus maze test; OFT: Open- field test; SEM: Standard error of the mean; SI: Social interaction.

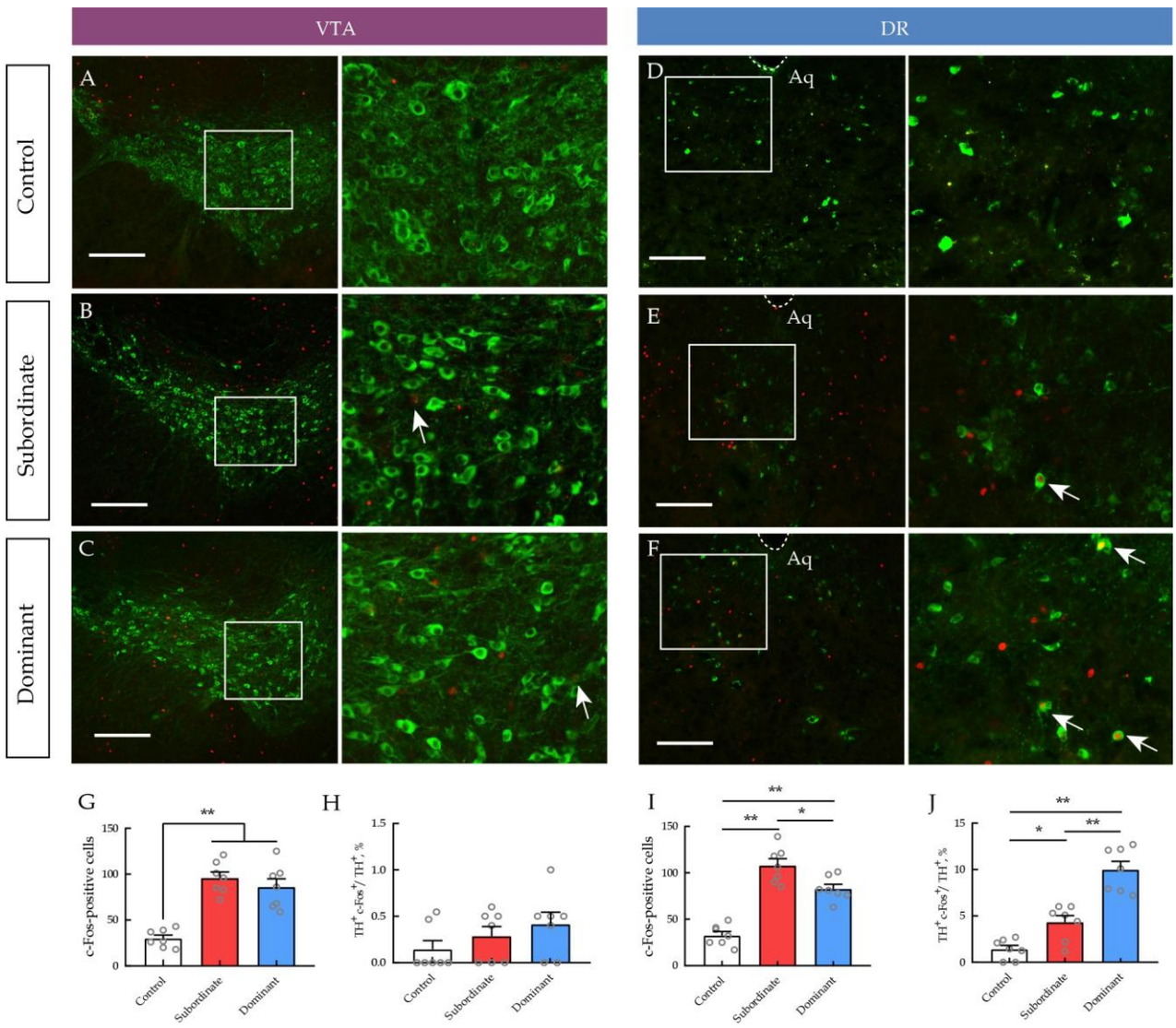

Figure 2 TH and c-Fos colocalization in the VTA and DR

A–F: Representative immunofluorescent images of c-Fos$^+$ (red dots) and TH$^+$ neurons (green cells) in the VTA and DR. White squares indicate position where the right column images were taken and arrows indicate double-labeled cells. Scale bars: 100 μm. G–J: Quantification of c-Fos and TH/c-Fos colocalization in the VTA and DR. Data are presented as mean±SEM, analyzed by one-way ANOVA. n=7 in each group. *: P<0.050; **: P<0.010. Aq: Aqueduct; DR: Dorsal raphe nucleus; SEM: Standard error of the mean; TH: Tyrosine hydroxylase; VTA: Ventral tegmental area.

Subsequent behavioral assays revealed selective effects on anxiety-like measures. In dominant mice, hM4D(Gi)-mediated inhibition significantly reduced time spent in the open arms in the EPM (Figure 5L, $F_{(2,21)}$=5.112, P=0.016; hM4D(Gi): Veh vs. CNO, P=0.047) and decreased the SI ratio in the SI test (Figure 5M, $F_{(2,21)}$=3.566, P=0.046; hM4D(Gi): Veh vs. CNO, P=0.013). In subordinate mice, hM3D(Gq)-mediated activation significantly increased time spent in the open arms in the EPM (Figure 5P, $F_{(2,21)}$=9.245, P<0.01; hM3D(Gq): Veh vs. CNO, P=0.021) but did not significantly affect the SI ratio in the SI test (Figure 5Q, $F_{(2,21)}$=0.311, P=0.736). Notably, these treatments did not significantly alter behavioral performance of either dominant or subordinate mice in the OFT (Figure 5J: $F_{(2,21)}$=1.375, P=0.275; Figure 5K: $F_{(2,21)}$=2.389, P=0.116; Figure 5N: $F_{(2,21)}$=1.308, P=0.319; Figure 5O: $F_{(2,21)}$=2.793, P=0.084). These findings indicate that while VTA DA neuron modulation does not significantly influence social rank, it can alter specific anxiety-related behaviors in a rank-dependent manner.

Inhibition of DR DA neurons lowers dominant rank and sociability, whereas activation of DR DA neurons increases subordinate rank and reduces anxiety

Targeted chemogenetic manipulations were next applied to DR DA neurons (Figure 6A). Validation of the viral strategy is provided in Supplementary Figure S4C, D, G, H. In the tube test, hM4D(Gi)-mediated inhibition of DR DA neurons in dominant mice significantly reduced their social rank (hM4D(Gi)+Veh vs. hM4D(Gi)+CNO, rank change rate: 62.5%, Fisher's exact test, P=0.026, Figure 6F). Conversely, hM3D(Gq)-mediated activation in subordinate mice significantly increased their social rank (hM3D(Gq)+Veh vs. hM3D(Gq)+CNO, rank change rate: 75%, Fisher's exact test, P<0.010, Figure 6H). Subsequent behavioral assays revealed that activation of DR DA neurons in subordinates significantly increased time spent in the open arms of the EPM (Figure 6P, $F_{(2,21)}$=9.303, P<0.01; hM3D(Gq): Veh vs. CNO, P=0.031), indicating reduced anxiety-like behavior. However, inhibition of DR DA neurons significantly reduced their SI ratio in the SI test

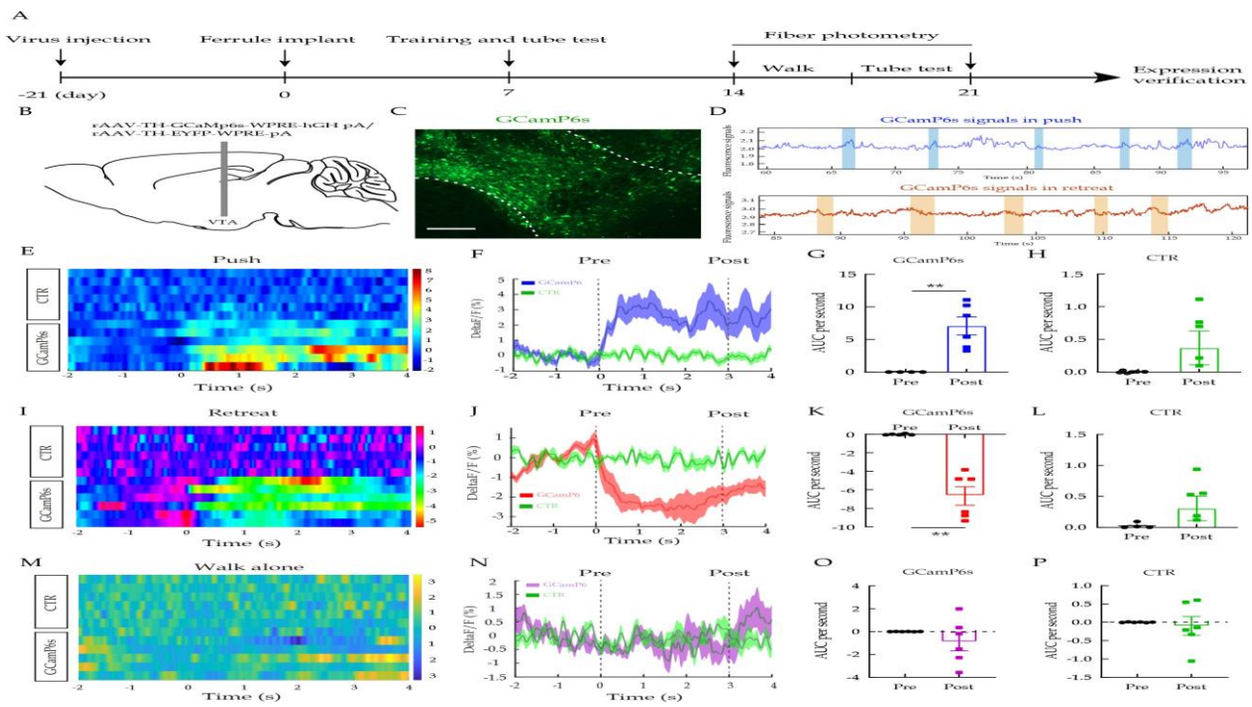

Figure 3 Fiber photometry recordings of VTA DA neurons during tube test

A: Study timeline. B: Viral injection strategy. C: Histology showing expression of GCaMP6s. Scale bar: 100 μm. D: Representative fluorescence changes of GCaMP6s during push and retreat. E, F, I, J, M, N: Heatmaps and peri-event plots of fluorescence signals aligned to onsets of push (E, F), retreat (I, J), and walk alone (M, N) in mice expressing GCaMP6s and control eGFP virus. In heatmap, different color bars represent different mice. In peri-event plot, line denotes mean signals of behaviors; shaded region denotes SE. n=18–24 trials from six mice. G, H, K, L, O, P: Quantification of changes in fluorescence signals before and after events in mice expressing GCaMP6s and control eGFP virus (G, H: Push; K, L: Retreat; O, P: Walk alone). Data are presented as mean±SEM, analyzed by paired t test. **: P<0.010. CTR: Control; DA: Dopamine; SEM: Standard error of the mean; TH: Tyrosine hydroxylase; VTA: Ventral tegmental area.

(Figure 6Q, $F_{(2,21)}$=7.297, P<0.01; hM4D(Gi): Veh vs. CNO, P=0.045). OFT performance was unaffected by either activation or inhibition of DR DA neurons in both dominant and subordinate mice (Figure 6J: $F_{(2,21)}$=2.836, P=0.081; Figure 6K:$F_{(2,21)}$=0.352, P=0.707; Figure 6N: $F_{(2,21)}$=0.362, P=0.701;

Figure 6O: $F_{(2,21)}$=2.349, P=0.120). These findings identify DR DA neurons as critical modulators of both social rank and specific socio-emotional behaviors in a rank-dependent manner.

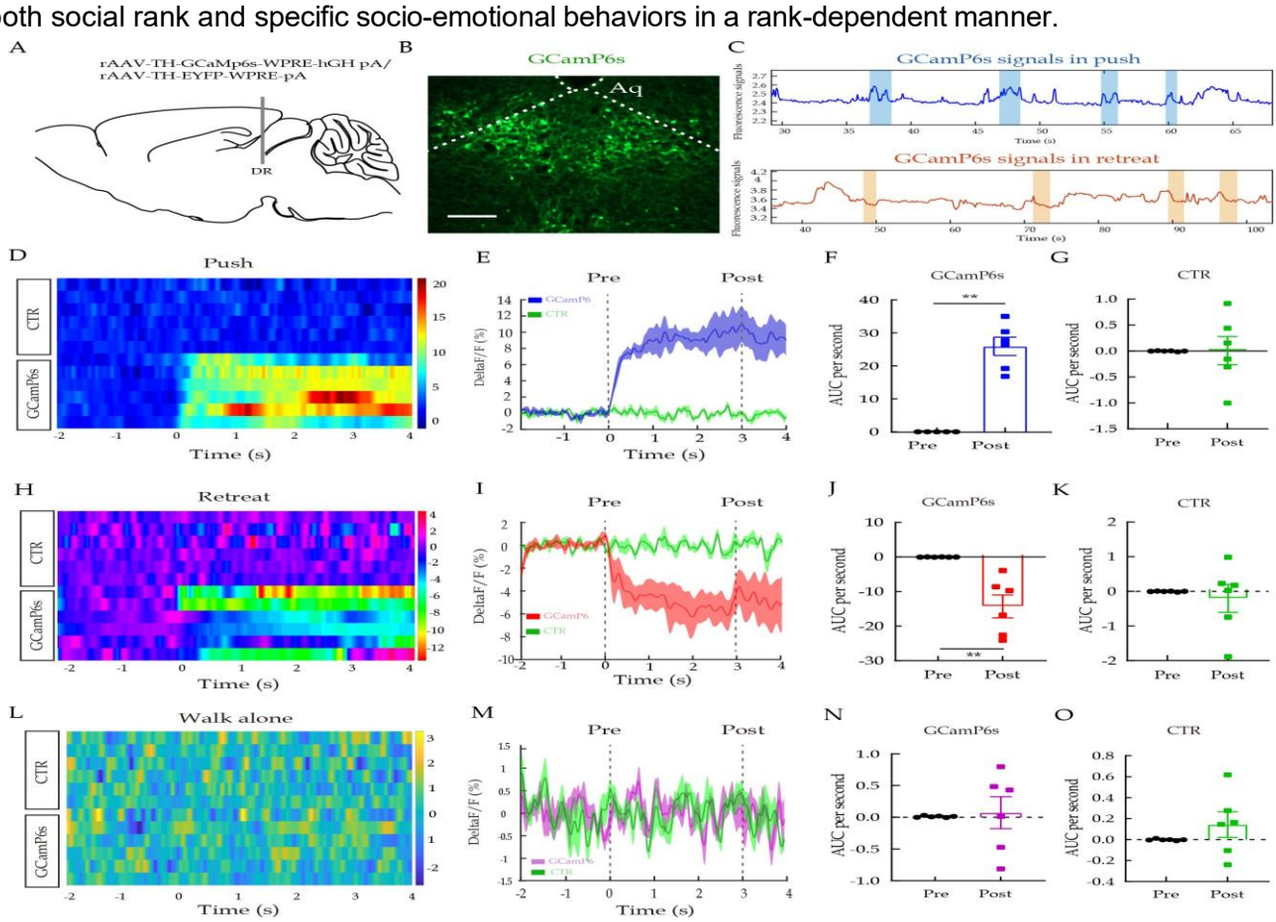

Figure 4 Fiber photometry recordings of DR DA neurons during tube test

A: Viral injection strategy. B: Histology showing expression of GCaMP6s. Scale bar: 100 μm. C: Representative fluorescence changes of GCaMP6s during push and retreat. D, E, H, I, L, M: Heatmaps and peri-event plots of fluorescence signals aligned to onsets of push (D, E), retreat (H, I), and walk alone (L, M) in mice expressing GCaMP6s and control eGFP virus. In heatmap, different color bars represent different mice. In peri-event plot, line denotes mean signals of behaviors; shaded region denotes SE. n=17–25 trials from six mice. F, G, J, K, N, O: Quantification of changes in fluorescence signals before and after events in mice expressing GCaMP6s and control eGFP virus (F, G: Push; J, K: Retreat; N, O: Walk alone). Data are presented as mean±SEM, analyzed by paired t test. **: P<0.010. CTR: Control; DA: Dopamine; DR: Dorsal raphe nucleus; SEM: Standard error of the mean; TH: Tyrosine hydroxylase.

DISCUSSION

This study delineated the distinct contributions of VTA and DR DA neurons to the regulation of social rank in mice. Through c-Fos profiling and fiber photometry, DR DA neurons in dominant mice exhibited heightened activity both during and following social encounters. Chemogenetic manipulation of these neurons bidirectionally altered dominance rank, establishing a direct causal role. In contrast, manipulation of VTA DA neurons failed to produce comparable effects, highlighting the region-specificity of dopaminergic circuits insocial hierarchy regulation. These findings position DR DA neurons, rather than VTA DA neurons, as a critical node in the neural architecture underlying social dominance in mice.

Consistent with previous studies (Battivelli et al., 2024b; Jiang et al., 2023; Xin et al., 2025; Xing et al., 2022; Zhang et al., 2022; Zhou et al., 2017), male C57BL/6 mice formed linear social hierarchies within a few days of co-housing (Figure 1C, D). Across behavioral assays, no significant rank-dependent differences were detected in anxiety-like behaviors or sociability (Figure 1E–J), aligning with findings from several

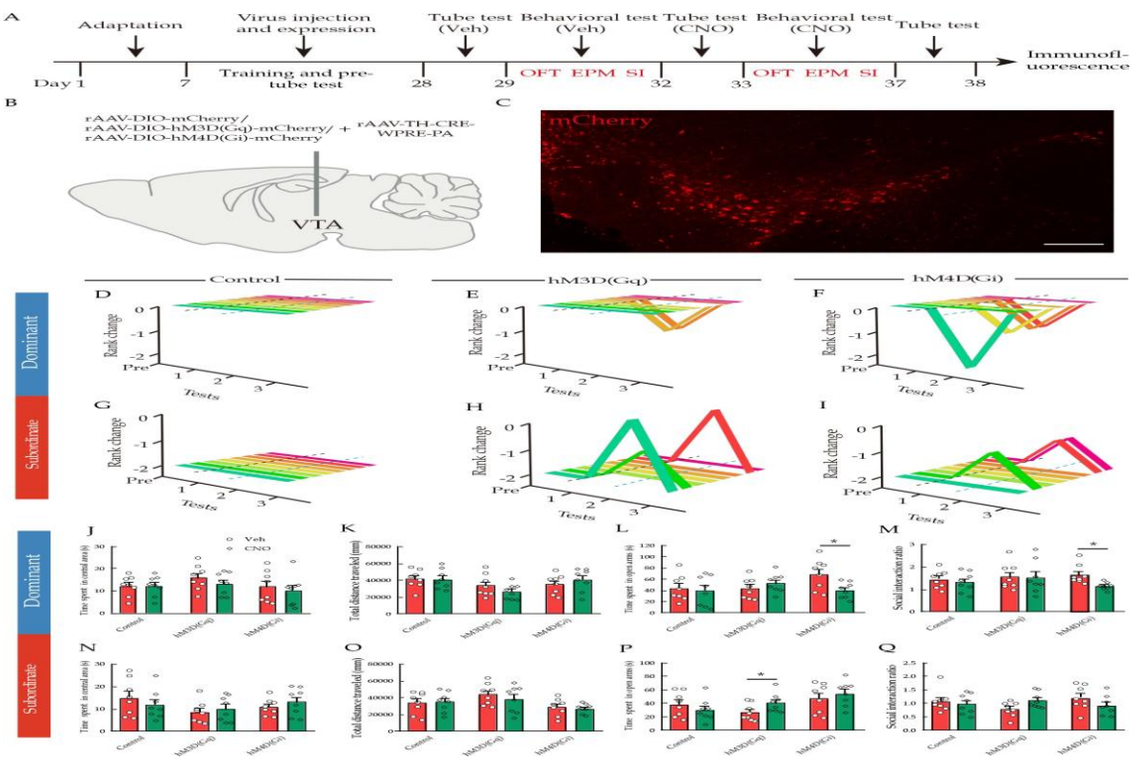

Figure 5 Chemogenetic modulation of VTA TH$^+$ neurons

A: Study timeline. B: Viral injection strategy. C: Immunohistochemical image showing DREADD expressions in the VTA, scale bar: 100 μm. D–I: Summary of rank changes in dominant (D–F) and subordinate (G–I) individuals. J, K, N, O: Time spent in the central zone and total distance traveled by dominant (J, K) and subordinate (N, O) individuals in OFT. L, P: Time spent in open arms by dominant (L) and subordinate (P) individuals in EPM. M, Q: SI ratio in dominant (M) and subordinate (Q) individuals in the three-chamber test. Data are presented as mean±SEM. n=8 in each group. *: P<0.050. Data in graph "D–I" analyzed by Fishers exact test, "J–Q" analyzed by two-way repeated-measures ANOVA. SI ratio: Social interaction ratio. CNO: Clozapine *N*-oxide; DREADDs: Designer receptors exclusively activated by designer drugs; EPM: Elevated plus maze test; OFT: Open-field test; SEM: Standard error of the mean; SI: Social interaction; TH: Tyrosine hydroxylase; Veh: Vehicle; VTA: Ventral tegmental area.

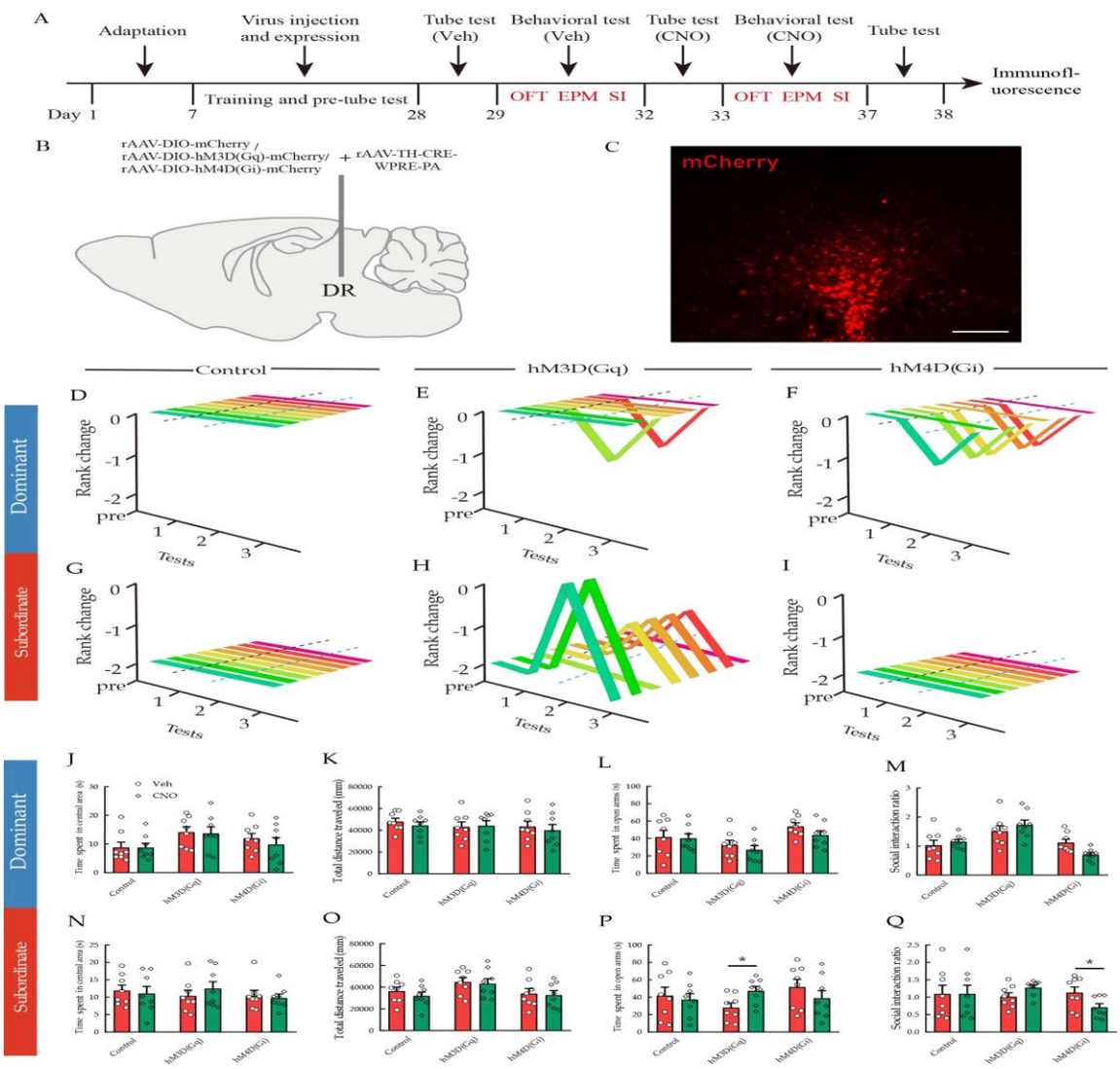

Figure 6 Chemogenetic modulation of DR TH⁺ neurons

A: Study timeline. B: Viral injection strategy. C: Immunohistochemical image showing DREADD expressions in the DR, scale bar: 100 μm. D–I: Summary of rank changes in dominant (D–F) and subordinate (G–I) individuals. J, K, N, O: Time spent in central zone and total distance traveled by dominant (J, K) and subordinate (N, O) individuals in OFT. L, P: Time spent in open arms by dominant (L) and subordinate (P) individuals in EPM. M, Q: SI ratio in dominant (M) and subordinate (Q) individuals in the three-chamber test. Data are presented as mean±SEM. n=8 in each group; *: P<0.050. Data in graph "D–I" analyzed by Fishers exact test, "J–Q" analyzed by two-way repeated-measures ANOVA. SI ratio: Social interaction ratio. CNO: Clozapine *N*-oxide; DR: Dorsal raphe nucleus; DREADDs: Designer receptors exclusively activated by designer drugs; EPM: Elevated plus maze test; OFT: Open-field test; SEM: Standard error of the mean; SI: Social interaction; TH: Tyrosine hydroxylase; Veh: Vehicle.

studies (Jiang et al., 2023; Varholick et al., 2018, 2021). However, other investigations have reported rank-related differences, with dominants exhibiting either increased (Battivelli et al., 2024b; Larrieu et al., 2017) or decreased anxiety (Horii et al., 2017; Song et al., 2023) and enhanced sociability (Kunkel & Wang, 2018; Li et al., 2023; Šabanović et al., 2020) compared to subordinates. Such discrepancies may reflect the inherent variability of behavioral phenotypes (Varholick et al., 2018, 2021), which are highly sensitive to external environments and physiological factors, such as test apparatus, light cycles, rearing conditions, and animal strains.

Dopaminergic signaling has long been implicated in social competition (Ghosal et al., 2019; Rillich & Stevenson, 2014), yet the specific contribution of VTA DA neurons remains a subject of debate. Optogenetic stimulation of VTA DA neurons has been shown to induce dominant behavior during competition for rewards (Lozano-Montes et al., 2019), and enhanced VTA DA activity via disinhibition has been linked to higher social dominance in rats (van der Kooij et al., 2018). In contrast, research has also shown that VTA DA neurons exhibit lower activity in dominant mice, with chemogenetic inhibition increasing social rank (Battivelli et al., 2024b). Similarly, in male mice, mPFC-NAc projections are reported to drive social winning, while mPFC-VTA projections promote social defeat (Choi et al., 2024). In the present study, VTA DA neurons exhibited phasic activation during active push behaviors and suppression during passive retreats in the tube test (Figure 3), yet chemogenetic manipulation of these neurons did not significantly affect social dominance (Figure 5). Moreover, c-Fos immunolabeling did not reveal increased VTA DA activity in dominant mice (Figure 2). These conflicting results may arise from methodological differences or selective targeting of distinct DA neuron subpopulations, which differ in molecular identity, connectivity, and functional specialization (Lammel et al., 2008). Future studies integrating subpopulation-specific targeting with *in vivo* single-unit recording may help resolve these circuit-level discrepancies.

Accumulating evidence suggests that DR DA neurons form a specialized midbrain DA subsystem, playing important regulatory roles in memory expression, opioid addiction, loneliness, depression, and arousal (Lin et al., 2021; Matthews et al., 2016; Wang et al., 2024). In the current study, DR DA neurons in dominant mice displayed heightened activity both during and after social competition in the tube test (Figure 2, Figure 4). Chemogenetic activation or inhibition of these neurons bidirectionally shifted dominance rank (Figure

6), providing direct causal evidence for their role in hierarchy regulation. Similarly, Xin et al. (2025) reported that stimulation of mPFC-DR projections promotes competitive success in the tube test, suggesting that DR DA neurons may be downstream targets of this pathway. However, verification of this hypothesis will require targeted connectivity analyses, such as monosynaptic tracing or cell-type-specific electrophysiology, to determine whether mPFC inputs directly engage DR DA neurons. Additionally, given that the DR is a principal serotonergic hub, the potential involvement of 5-HT or other neuronal types cannot be excluded, particularly in light of evidence that mPFC projections preferentially innervate 5-HTergic populations (Weissbourd et al., 2014). Furthermore, whether baseline DR DA activity differs between dominant and subordinate individuals remains unclear—a question that could be resolved through *in vivo* electrophysiological recordings in freely behaving animals.Manipulation of VTA and DR DA neurons also modulated anxiety-like and social behaviors. In the EPM test, VTA DA inhibition increased anxiety-like behavior and reduced sociability, particularly in dominant individuals (Figure 5L, M), whereas activation produced an anxiolytic effect (Figure 5P). These findings are consistent with previous studies on VTA DA neurons (Bariselli et al., 2018; Zweifel et al., 2011). For DR DA neurons, chemogenetic activation increased open-arm exploration in subordinates during the EPM test (Figure 6P), consistent with reduced anxiety-like behavior, whereas inhibition decreased the SI ratio (Figure 6Q). In contrast, manipulation of DR DA neurons did not significantly alter anxiety or sociability in dominant individuals (Figure 6L, M). Prior studies reveal similarly complex and context-dependent effects: Taylor et al. (2019) reported that DR DA activation produced profound analgesia without changes in anxiety, while Matthews et al. (2016) found that optogenetic activation induced a loneliness-like state that enhanced sociability in the three-chamber test, with photoinhibition producing the opposite effect. These observed discrepancies suggest that social experience, particularly hierarchical status, may strongly influence the behavioral outcomes of DR DA neuron manipulation, potentially reshaping their functional role in socio-emotional processing.

Unlike VTA DA neurons which send extensive projections to the limbic and cortical regions, DR DA neurons display a more restricted projection pattern, primarily targeting the CeA and BNST (Lin et al., 2020). This anatomical distinction underscores the need for future studies to delineate the precise neural pathways underlying social hierarchy formation. Furthermore, DA is known to exert its effects via two major receptor subtypes, D1-like (D1Rs) and D2-like (D2Rs), which differ in intracellular signaling cascades and functional outcomes (Li et al., 2023; Liu et al., 2021). Systematic investigation of their respective contributions to social dominance within downstream projection targets is also warranted.

Our immunofluorescence analyses revealed significant c- Fos activation in both the VTA and DR following tube test- based social competition in dominant and subordinate mice (Figure 2G, I). Double-labeling analyses further demonstrated that c-Fos activation was selectively elevated in DR DA neurons of dominant individuals (Figure 2J) but not in VTA DA neurons of either rank group (Figure 2H). Given that c-Fos is a broad marker of neuronal activity and does not necessarily correlate with specific behavioral outputs, these findings suggest that other neuronal types may also contribute to social competition-related behaviors, including anxiety-like responses—a hypothesis that merits targeted investigation in future studies.

Overall, the current study identified DR DA neurons as key modulators of social hierarchy in mice. Nevertheless, several limitations

should be noted. First, although the majority of virally transduced cells were TH^+, potential off-target infection of other neuronal populations cannot be excluded as a confounding variable. Second, social dominance was not corroborated using complementary behavioral paradigms, such as the warm spot or scent-marking tests, despite the tube test being extensively validated for this purpose in previous studies (Fan et al., 2019; Larrieu et al., 2017). Furthermore, considering the current gap between neuroscience and ethology (Battivelli et al., 2024a; Murlanova et al., 2022), future studies should incorporate more ethologically relevant approaches, such as employing wild- derived strains and determining dominant-subordinate relationships under semi-natural conditions over extended time periods, to better validate and contextualize the findings. Third, the study was conducted in triads of male mice, leaving the generalizability of these findings to larger groups or female cohorts unresolved. Finally, although chemogenetic modulation of social rank produced more robust effects in the DR, some individuals also exhibited changes following VTA modulation. Studies with larger sample sizes may yield different conclusions. Despite these limitations, this study provides new insights into the neurochemical mechanisms governing social dominance.

REFERENCES

El Rawas R, Hofer A, and Amaral IM. 2021. Is it feasible to get up to the top rank? special emphasis on cocaine misuse and the mesolimbic dopaminergic system. 9(8): 877 in Biomedicines.

Hörnberg H, Prévost-Solié C, Bariselli S, et al. (2018). Neuroligin 3 and VTA dopamine neurons play a part in sociability qualities associated with unfamiliar conspecific interaction. 9(1): 3173 in Nature Communications.

Fan ZX, Hu HL, Battivelli D, et al. 2024a. How can the neuroscience of aggression, fear, and dominance be informed by ethology? Neuroscience Reviews in Nature, 25(12): 809–819.

Conabady E, Battivelli D, Vernochet C, et al. 2024b. Stress signaling and dopamine neuron activity as connections between sensitivity to psychopathology and social hierarchy. 774–784 in Biological Psychiatry, 95(8).

Robinson JE, Treweek JB, Cho JR, et al. 2017. By responding to salient stimuli, dopamine neurons in the dorsal raphe influence arousal and encourage alertness. Neuron, 94(6): 1205–1219. e8.

In 2024, Choi TY, Jeon H, Jeong S, et al. On the other hand, distinct transcriptional states and prefrontal projection activity coordinate social hierarchy and competitiveness. 112(4): 611–627. e8; Neuron.

Curley JP, Tye KM, Dwortz MF, et al. 2022. neural networks that make social rank representation easier. Biological Sciences, 377(1845): 20200444, Philosophical Transactions of the Royal Society B.

Chang JR, Liang YL, Fan ZX, et al. (2023). neural process that underlies the depressive-like mood linked to a decline in social standing. e17; Cell, 186(3): 560–576.

Zhu H, Zhou TT, Fan ZX, et al. 2019. assessing mice's social structure using the tube test. 14(3), Nature Protocols, 819–831.

Grossouw LM, Garritsen O, van Battum EY, et al. 2023. Subtypes of dopamine neurons: their development, wiring, and function. 134–152 in Nature Reviews Neuroscience, 24(3).

Neuropharmacology of the mesolimbic system and related circuits on social hierarchies, Ghosal S, Sandi C, van der Kooij MA. 2019. 107498 in Neuropharmacology, 159.Sakakibara H, Horii Y, Nagasawa T, et al. 2017. Group-housed animals' behavior and gene expression are influenced by the hierarchy in their home cage. C57BL/6 male mice. *Scientific Reports*, **7**(1): 6991.

Janet R, Ligneul R, Losecaat-Vermeer AB, et al. 2022. Regulation of social hierarchy

learning by serotonin transporter availability. *Neuropsychopharmacology*, **47**(13): 2205–2212.

Jiang Y, Zhou J, Song BL, et al. 2023. 5-HT1A receptor in the central amygdala and 5-HT2A receptor in the basolateral amygdala are involved in social hierarchy in male mice. *European Journal of Pharmacology*, **957**: 176027.

Johnson SL, Leedom LJ, Muhtadie L. 2012. The dominance behavioral system and psychopathology: evidence from self-report, observational, and biological studies. *Psychological Bulletin*, **138**(4): 692–743.

Kaplan JR, Manuck SB, Fontenot MB, et al. 2002. Central nervous system monoamine correlates of social dominance in cynomolgus monkeys (*Macaca fascicularis*). *Neuropsychopharmacology*, **26**(4): 431–443.

Kunkel T, Wang HB. 2018. Socially dominant mice in C57BL6 background show increased social motivation. *Behavioural Brain Research*, **336**: 173–176.

Lammel S, Hetzel A, Häckel O, et al. 2008. Unique properties of mesoprefrontal neurons within a dual mesocorticolimbic dopamine system. *Neuron*, **57**(5): 760–773.

Larrieu T, Cherix A, Duque A, et al. 2017. Hierarchical status predicts behavioral vulnerability and nucleus accumbens metabolic profile following chronic social defeat stress. *Current Biology*, **27**(14): 2202–2210. e4.

Leclair KB, Russo SJ. 2021. Using social rank as the lens to focus on the neural circuitry driving stress coping styles. *Current Opinion in Neurobiology*, **68**: 167–180.

Li LF, Li ZL, Song BL, et al. 2023. Dopamine D2 receptors in the dorsomedial prefrontal cortex modulate social hierarchy in male mice. *Current Zoology*, **69**(6): 682–693.

Lin R, Liang JM, Luo MM. 2021. The raphe dopamine system: roles in salience encoding, memory expression, and addiction. *Trends in Neurosciences*, **44**(5): 366–377.

Lin R, Liang JM, Wang RY, et al. 2020. The raphe dopamine system controls the expression of incentive memory. *Neuron*, **106**(3): 498–514. e8. Liu CL, Goel P, Kaeser PS. 2021. Spatial and temporal scales of dopamine transmission. *Nature Reviews Neuroscience*, **22**(6): 345–358.

Lozano-Montes L, Astori S, Abad S, et al. 2019. Latency to reward predicts social dominance in rats: a causal role for the dopaminergic mesolimbic system. *Frontiers in Behavioral Neuroscience*, **13**: 69.

Liu YJ, Jiang Y, Bai YT, et al. 2025. Serotonergic modulation of social dominance via the dorsal raphe-central amygdala circuit in male mice. *Integrative Zoology*, doi: 10.1111/1749-4877.70003.

Madigan A, Daly M. 2023. Socioeconomic status and depressive symptoms and suicidality: the role of subjective social status. *Journal of Affective Disorders*, **326**: 36–43.

Martinez D, Orlowska D, Narendran R, et al. 2010. Dopamine type 2/3 receptor availability in the striatum and social status in human volunteers. *Biological Psychiatry*, **67**(3): 275–278.

Matthews GA, Nieh EH, Vander Weele CM, et

al. 2016. Dorsal raphe dopamine neurons represent the experience of social isolation. *Cell*, **164**(4): 617–631.

Murlanova K, Kirby M, Libergod L, et al. 2022. Multidimensional nature of dominant behavior: insights from behavioral neuroscience. *Neuroscience & Biobehavioral Reviews*, **132**: 603–620.

Qu C, Ligneul R, Van der Henst JB, et al. 2017. An integrative interdisciplinary perspective on social dominance hierarchies. *Trends in Cognitive Sciences*, **21**(11): 893–908.

Rillich J, Stevenson PA. 2014. A fighter's comeback: dopamine is necessary for recovery of aggression after social defeat in crickets. *Hormones and Behavior*, **66**(4): 696–704.

Šabanović M, Liu H, Mlambo V, et al. 2020. What it takes to be at the top: